



Multistage Kondo effect in a multiterminal geometry: A modular quantum interferometer

D. B. Karki

*Division of Quantum State of Matter, Beijing Academy of Quantum Information Sciences, Beijing 100193, China*Andrei I. Pavlov  and Mikhail N. Kiselev *The Abdus Salam International Centre for Theoretical Physics (ICTP), Strada Costiera 11, I-34151 Trieste, Italy*

(Received 25 October 2021; revised 21 December 2021; accepted 11 January 2022; published 21 January 2022)

Quantum systems characterized by an interplay between several resonance scattering channels demonstrate very rich physics. To illustrate it we consider a multistage Kondo effect in nanodevices as a paradigmatic model for a multimode resonance scattering. We show that the channel crosstalk results in a destructive interference between the modes. This interplay can be controlled by manipulating the tunneling junctions in the multilevel and multiterminal geometry. We present a full-fledged theory of the multistage Kondo effect at the strong-coupling Fermi-liquid fixed point and discuss the influence of quantum interference effects to the quantum transport observables.

DOI: [10.1103/PhysRevB.105.L041410](https://doi.org/10.1103/PhysRevB.105.L041410)

Introduction. The exchange coupling between a localized spin and conduction electrons at low temperature gives rise to the Kondo screening phenomenon [1–3]. This phenomenon has been extensively studied over decades and often serves as a test bed of strongly correlated physics [4]. Depending on the size of the localized spin S and the number of conduction channels \mathcal{K} , the ground state of the system falls into one of three classes, often referred as fully screened ($\mathcal{K} = 2S$), underscreened ($\mathcal{K} < 2S$), and overscreened ($\mathcal{K} > 2S$) cases [5]. Among them, the fully screened and underscreened Kondo effects are completely described by a local Fermi-liquid (FL) theory [2]. Recently, remarkable progress was achieved in controllable realizations of various fully screened Kondo phenomena in nanostructures [6,7], further fuelling the continued interests in this field. With the two-stage Kondo effect being now a subject of experimental studies, it is now a question if more general multiterminal setups can contain principally new and richer physics in comparison to the currently realized ones.

The fully screened Kondo effect, although described by FL theory, possesses several exotic properties beyond its trivial generalization of a single channel, corresponding to $S = 1/2$ and $\mathcal{K} = 1$ [4,8]. The $S = 1/2$ Kondo effect is unlikely to be sufficient for the complete description of the physics of a magnetic impurity in a nonmagnetic host since the truncation of the impurity spectrum to one level is not possible [9]. Thus, the consistent description requires the consideration of several orbitals of conduction electrons $\mathcal{K} > 1$ which interact with the higher-spin $S > 1/2$ of the localized magnetic impurity [10–12]. The recent experiment [7] has further shed light on the relevance of high-spin Kondo effects in nanostructures. In addition, with the rapid progress of semiconductor quantum dot technologies, the understanding and control over the high-spin state properties have been quickly expanding in recent years with the ambition of using high-spin states for quantum information processing [13].

The prototypical example of multichannel fully screened Kondo effects corresponds to the case of $S = 1$ impurity coupled to $\mathcal{K} = 2$ conduction channels. It is well known that the two-terminal (2T) setup offers, as maximum, two distinct channels built as the linear combinations (symmetric and antisymmetric) of electron states in the left (L) and right (R) terminal. These channels will be referred to without loss of generality as even and odd channels, respectively [14]. Based on the ways of how to realize $\mathcal{K} = 2$, two different cases of the $S = 1$ Kondo effect emerge. The first case corresponds to a 2T realization with an explicit coupling between the even and odd channels in order to have $\mathcal{K} = 2$. The other case is achieved by using capacitively coupled four terminals (two pairs of left and right leads) to provide two Kondo channels (one channel from each pair of terminals) necessary for the screening of the $S = 1$ impurity [15–20]. While the strong-coupling regime of the former case results in completely destructive interference [18], the latter one allows us to have fully constructive interferences [15]. These two cases are commonly referred to as series and parallel configurations of two-stage Kondo effects and are detailed in Fig. 1 (top). The series configuration results in completely destructive interference due to the competition between two Kondo channels, both being at resonant scattering (even and odd channels characterized by respective Kondo temperatures T_K^e and T_K^o). This configuration is known to possess nonmonotonic conductance [Fig. 1 (bottom)]—a benchmark property for observations of two-stage Kondo (2SK) effects [9].

Multi ($N > 2$)-terminal nanodevices have attracted great attention from both theoretical and experimental communities for their potential use in nanotechnologies [21–24]. In addition, probing several hallmarks of strongly correlated electron systems, such as the Kondo density of states, requires a setup beyond 2T [25]. Likewise, the experimental detection of Hanbury Brown–Twiss (HBT) correlations requires a minimal setup of 3T geometry [26]. Moreover, certain classes of Kondo

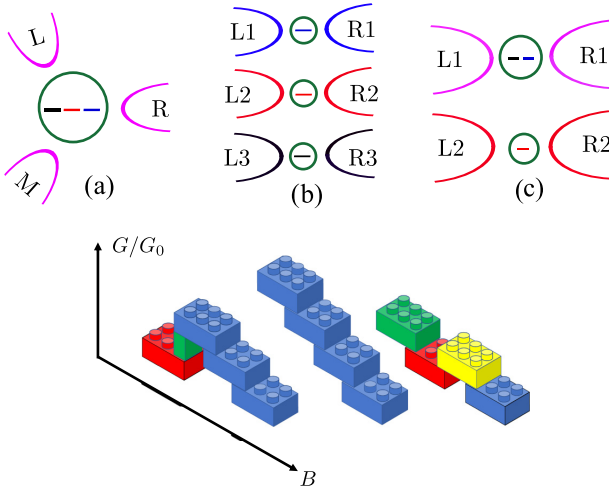


FIG. 1. Top: The schematic representation of three-channel $S = 3/2$ Kondo setups studied in this Letter. (a) The series configuration exhibiting 3SK effects via three interfering channels, (b) the capacitively coupled system forming a parallel configuration for $S = 3/2$ Kondo effects with decoupled resonant channels, and (c) a hybrid Kondo setup allowing for the study of the interplay between multistage and single-stage Kondo effects (see text for details). Bottom: Cartoon for the schematic dependence of the differential conductance on a magnetic field for (a)–(c) setups. Blue “ascending” modular blocks denote different stages of Kondo screening. Red “descending” modular blocks stand for effects of destructive interference. Yellow and green modular blocks are used to highlight the nonmonotonicity.

effects, such as the topological Kondo effects, are intrinsically multiterminal effects [27]. Interestingly, the physics of the $S = 1/2$ Kondo impurity coupled to N terminals can be reached by mapping it to the corresponding two-terminal situation since only the even channel is coupled to the impurity [28]. In contrast, the N -terminal Kondo effect with $S = N/2$ exhibiting a fully screened ground state couples all $N = \mathcal{K}$ conduction modes to the impurity degrees of freedom, resulting in multiresonant Kondo screening phenomena [18].

We now turn our attention to the simplest situation of $S = 3/2$ and $\mathcal{K} = 3$. While the corresponding parallel configuration needs six terminals, the series setup requires three terminals (3T). In addition, it is evident that the higher-spin parallel configuration is a trivial generalization of the corresponding $S = 1/2$ situation [17]. Our focus would thus be on the series configuration where the nontrivial interplay between three Kondo channels provides far richer physics over the widely studied two-stage Kondo effects. In this case, one symmetric mode (e) and two modes orthogonal to the even mode (o1 and o2) compete with each other to screen the localized spin $S = 3/2$. These three channels are characterized by three Kondo temperatures which can be tuned to satisfy a certain hierarchy $T_K^e \geq T_K^{o1} \geq T_K^{o2}$ (see below). The fully screened Kondo ground state, the Kondo singlet, would then result from three different stages of screening $S = 3/2 \rightarrow 1 \rightarrow 1/2 \rightarrow 0$. We refer to this phenomenon as the three-stage Kondo (3SK) effect and concentrate our work on the development of low-energy FL theory of transport through the 3SK effect.

Formulation of problem. We consider a multilevel quantum impurity (dot) with an effective spin S coupled to N external

terminals. The high-spin state of the dot is achieved by the Hund’s coupling (see Ref. [29] for details) in the presence of an external Zeeman field B . This system is represented by the generic Anderson model [30,31]

$$H = \sum_{k\alpha\sigma} (\epsilon_k + \epsilon_\sigma^Z) C_{\alpha k\sigma}^\dagger C_{\alpha k\sigma} + \sum_{\alpha k i \sigma} t_{\alpha i} C_{\alpha k\sigma}^\dagger d_{i\sigma} + \text{H.c.} + \sum_{i\sigma} (\epsilon_i + \epsilon_\sigma^Z) d_{i\sigma}^\dagger d_{i\sigma} + E_c \hat{N}^2 - \mathcal{I} \hat{S}^2, \quad (1)$$

where $C_{\alpha k\sigma}$ annihilates an electron at the terminal α from the momentum state k with spin σ ($=\uparrow, \downarrow$) and $\epsilon_k = \epsilon_k - \mu$ is the energy of conduction electrons with respect to the chemical potential μ . The electron in the i th orbital of the quantum dot with energy $\epsilon_i + \epsilon_\sigma^Z$ ($\epsilon_\sigma^Z = -\sigma B/2$) is described by the operator $d_{i\sigma}$ such that $\hat{N} = \sum_{i\sigma} d_{i\sigma}^\dagger d_{i\sigma}$ represents the total number of electrons in the dot. The exchange integral accounting for the Hund’s rule is represented by \mathcal{I} , E_c is the charging energy such that $\mathcal{I} \ll E_c$, and $t_{\alpha i}$ are the tunneling matrix elements (for details, see Refs. [32–34]).

Achieving multiple resonant Kondo channels. As the relevant case of the 3SK effects, we concentrate our discussion on the particular case of a three-level impurity ($i = 1, 2, 3$) tunnel-coupled to three external leads: left (L), middle (M), and right (R) (see Fig. 1). Assuming a total of three electrons, the presence of Hund’s coupling results in the quartet configuration of the impurity possessing an effective spin $S = 3/2$. We note that the spin-3/2 quartet state is well separated from the corresponding spin-1/2 doublets [see Supplemental Material (SM) [35] for details]. We then apply the Schrieffer-Wolff transformation [36] to Eq. (1) which eliminates the charge fluctuations between the orbitals resulting in the effective Hamiltonian as

$$\mathcal{H} = \mathcal{H}_0 + \frac{1}{2} \sum_{\alpha, \alpha'=1}^3 \sum_{k\sigma, k'\sigma'} \mathcal{J}_{\alpha\alpha'} S \cdot C_{\alpha k\sigma}^\dagger \tau_{\sigma\sigma'} C_{\alpha' k'\sigma'}, \quad (2)$$

with $\mathcal{H}_0 = \sum_{\alpha k\sigma} \epsilon_k C_{\alpha k\sigma}^\dagger C_{\alpha k\sigma}$ and $\tau_{\sigma\sigma'}$ being the Pauli matrix. The 3×3 Hermitian matrix \mathbb{J} of exchange couplings $\mathcal{J}_{\alpha\alpha'}$ can be expressed in terms of the size of the effective spin S , charging energy E_c , and nine complex tunneling elements $t_{\alpha i}$ such that

$$\mathcal{J}_{\alpha\alpha'} = \frac{2}{SE_c} \sum_{i=1}^3 t_{\alpha i}^* t_{\alpha' i}. \quad (3)$$

The 3×3 matrix \mathbb{J} possesses at most three nonzero eigenvalues, each representing distinct conduction channels [37], let us say $\mathcal{J}_{1,2,3}$. To achieve $\mathcal{J}_{1,2,3} > 0$, the matrix \mathbb{J} must possess the following three invariants $\mathcal{M}_{1,2,3}$ such that

$$\begin{aligned} \mathcal{M}_1 &= \text{Tr } \mathbb{J} = \sum_{i=1}^3 \mathcal{J}_i > 0, & \mathcal{M}_2 &= \text{Det } \mathbb{J} = \prod_{i=1}^3 \mathcal{J}_i > 0, \\ \mathcal{M}_3 &= \frac{1}{2} [(\text{Tr } \mathbb{J})^2 - \text{Tr } \mathbb{J}^2] = \mathcal{J}_1 \mathcal{J}_2 + \mathcal{J}_2 \mathcal{J}_3 + \mathcal{J}_1 \mathcal{J}_3 > 0, \end{aligned}$$

where “Tr” and “Det” stand for the trace and determinant, respectively. The simplest case arises when all $t_{\alpha i}$ are tuned to be equal where \mathbb{J} permits only one eigenvalue, with the other two being zero since for this case $\mathcal{M}_2 = 0$. The resulting situation describes the single-channel underscreened ($S > \mathcal{K} = 1$)

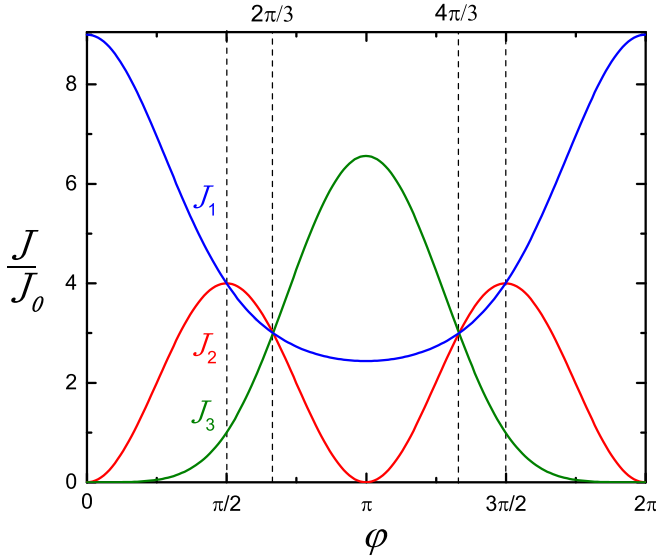


FIG. 2. The phase tunable eigenvalues of exchange matrix \mathbb{J} providing three distinct Kondo channels (see text for details).

Kondo effects characterized by the channel corresponding to the single nonzero eigenvalue of \mathbb{J} .

The complex tunneling parameters $t_{\alpha i} = |t_{\alpha i}|e^{i\varphi_{\alpha i}}$ provide a very large parameter space and hence various \mathbb{J} matrices can be formed. For a simple demonstration of the 3SK effect, one needs all three eigenvalues of \mathbb{J} to be nonzero and positive definite since these eigenvalues will provide independent conduction channels for the Kondo screening. One of the simplest ways to achieve such a goal is to consider a single phase $\varphi \neq 0$ keeping all tunneling amplitudes the same, satisfying the condition $\mathcal{M}_{1,2,3} > 0$. To this end, we chose a prototypical realization such that the tunneling elements are parametrized as [35]

$$\begin{aligned} t_{L1} &= |t|e^{i\varphi}, & t_{L2} &= |t|, & t_{L3} &= |t|e^{-i\varphi}, \\ t_{M1} &= |t|e^{-i\varphi}, & t_{M2} &= |t|, & t_{M3} &= |t|e^{i\varphi}, \\ t_{R1} &= t_{R2} = t_{R3} = |t|. \end{aligned} \quad (4)$$

This choice results in three eigenvalues $\mathcal{J}_{1,2,3}$ of the \mathbb{J} matrix which can be tuned with phase φ ,

$$\begin{aligned} \mathcal{J}_{1,3} &= \frac{\mathcal{J}_0}{2} [7 + 2 \cos 2\varphi \pm \sqrt{32 \cos \varphi + (5 + 2 \cos 2\varphi)^2}], \\ \mathcal{J}_2 &= 4\mathcal{J}_0 \sin^2 \varphi, \end{aligned} \quad (5)$$

where we denoted $\mathcal{J}_0 = \frac{2|t|^2}{S E_c}$. It is seen from the above equation that $\varphi = 0$ results in $\mathcal{J}_1 > 0$ with $\mathcal{J}_{2,3} = 0$. Thus, by tuning the phase $\varphi \in [0, 2\pi)$, one can explicitly achieve the desirable condition $\mathcal{J}_{1,2,3} > 0$ which gives three distinct Kondo channels, see Fig. 2. In addition, tuning φ further offers some interesting points where two eigenvalues are equal, as well as all of them being equal, keeping the condition $\mathcal{J}_{1,2,3} \neq 0$. This provides a viable way of manipulating the strength of the conduction channels. In addition, as detailed in SM [35], $\mathcal{J}_{1,2,3} > 0$ can be achieved even with $\varphi = 0$ (the real tunneling elements) by considering asymmetry among the tunneling amplitudes. Therefore, in the following discussion

we assume without loss of generality that all three eigenvalues of the matrix \mathbb{J} are positive and hence all scattering channels interact with the quantum impurity.

Rotation of electron states in the leads. The usual situation of 2T geometry always suggests the rotation of electron states given by the Glazman-Raikh (GR) transformation [14] [for symmetric coupling it writes $C_e \equiv (C_L + C_R)/\sqrt{2}$ and $C_o \equiv (C_L - C_R)/\sqrt{2}$], which paves the way of writing Hamiltonian Eq. (2) in diagonal form and hence resulting in a Kondo Hamiltonian. Increasing the number of terminals N but keeping only one nonzero eigenvalue of \mathbb{J} is the trivial case since only the symmetric mode $C_e = \sum_{\alpha} C_{\alpha}/\sqrt{N}$ would be coupled to the impurity, with all other $N - 1$ modes orthogonal to C_e remaining completely decoupled. Therefore for N -terminal geometry with all eigenvalues of \mathbb{J} being nonzero, a transformation similar to GR is more involved. Interestingly, the remaining $N - 1$ rotated states which are orthogonal to C_e can be formed by using the $N - 1$ Cartan generators of the $SU(N)$ group [8,23,38]. For the particular case of 3T geometry, the remaining two rotated states are formed by using the generators of the Cartan basis of the $SU(3)$ representation, namely $\lambda_3/\sqrt{2}$ and $\lambda_8/\sqrt{2}$.

A naive rotation transformation constructed from C_e , $C_{o1} \leftrightarrow \lambda_3/\sqrt{2}$, and $C_{o2} \leftrightarrow \lambda_8/\sqrt{2}$ [39],

$$\begin{pmatrix} C_e \\ C_{o1} \\ C_{o2} \end{pmatrix} = \mathbb{U}_{\lambda} \begin{pmatrix} C_L \\ C_M \\ C_R \end{pmatrix}, \quad \mathbb{U}_{\lambda} = \begin{pmatrix} \frac{1}{\sqrt{3}} & \frac{1}{\sqrt{3}} & \frac{1}{\sqrt{3}} \\ -\frac{1}{\sqrt{2}} & \frac{1}{\sqrt{2}} & 0 \\ -\frac{1}{\sqrt{6}} & -\frac{1}{\sqrt{6}} & \frac{2}{\sqrt{6}} \end{pmatrix}, \quad (6)$$

would neither contain the coupling asymmetry $|t_{\alpha i}| \neq |t|_{\alpha' i'}$ nor the information about the tunneling phase $\varphi \neq 0$. We thus find a very general transformation \mathbb{U} (similar to GR rotation in 2T geometry) for 3T Kondo geometry which provides all eigenvalues of \mathbb{J} to be positive nonzeros $\mathcal{J}_{1,2,3} > 0$ by accounting for the tunneling asymmetry and phase. We relegate the discussion of this general transformation to the SM [35] and concentrate our discussion here to the case of having the same tunneling amplitudes $|t|_{\alpha i}$ but with $\varphi \neq 0$. As detailed in the SM, the most general transformation accounting for the choice of Eq. (4) reads

$$\mathbb{U}[\mathcal{C}(\varphi)] = \frac{2}{\sqrt{8 + (\mathcal{C} + 2)^2}} \times \overline{\mathbb{U}}[\mathcal{C}(\varphi)], \quad (7)$$

with

$$\overline{\mathbb{U}} = \begin{pmatrix} 1 & 1 & 1 + \frac{\mathcal{C}}{2} \\ -\sqrt{\frac{3}{2}}\sqrt{1 + \frac{\mathcal{C}}{12}(\mathcal{C} + 4)} & \sqrt{\frac{3}{2}}\sqrt{1 + \frac{\mathcal{C}}{12}(\mathcal{C} + 4)} & 0 \\ -\frac{1}{\sqrt{2}}(1 + \frac{\mathcal{C}}{2}) & -\frac{1}{\sqrt{2}}(1 + \frac{\mathcal{C}}{2}) & \sqrt{2} \end{pmatrix},$$

$$\mathcal{C}(\varphi) = \sqrt{11 - 4 \cos(\varphi) + 2 \cos(2\varphi)} - 1 - 2 \cos(\varphi), \quad \mathcal{C}(0) = 0.$$

With the help of the unitary matrix \mathbb{U} Eq. (7) we write the Hamiltonian Eq. (2) in diagonal form. The resulting Kondo Hamiltonian reads

$$\mathcal{H}_K = \sum_a (\mathcal{H}_0^a + \mathcal{J}_a \mathbf{s}_a \cdot \mathbf{S}), \quad (8)$$

where $a = e, o1, o2$ are the channel indices and \mathbf{s}_a stands for the spin-density operator in the new basis a . In addition, three

nonzero eigenvalues (for $\varphi \neq 0$) of \mathbb{J} have been relabeled as $\mathcal{J}_1 = \mathcal{J}_e$, $\mathcal{J}_2 = \mathcal{J}_{o1}$, and $\mathcal{J}_3 = \mathcal{J}_{o2}$.

Kondo temperatures. Going beyond the second order of the Schrieffer-Wolff transformation results in an interaction among difference channels which reads [18]

$$\mathcal{H}_{\text{ch-int}} = - \sum_{a,b:a \neq b} \mathcal{J}_{ab} \mathbf{s}_a \cdot \mathbf{s}_b. \quad (9)$$

While the amplitude of \mathcal{J}_a (as seen earlier) scales with $\sim |t|^2/E_c$, the ferromagnetic coupling among different channels \mathcal{J}_{ab} scales as $\sim \mathcal{J}_a \mathcal{J}_b/E_c$ [18]. Therefore, Eq. (9) becomes irrelevant in the weak-coupling regime, which allows us to define three distinct Kondo temperatures characterizing three different conduction channels,

$$T_K^a = D \exp \left[-\frac{1}{2\nu_F \mathcal{J}_a} \right], \quad (10)$$

where D is a bandwidth and ν_F is the three-dimensional electron density of states in the leads. Since $\mathcal{J}_a(\varphi)$ are tuned through φ , we may express the Kondo temperature as $T_K^a \equiv T_K^a(\varphi)$, resulting in the least exotic situation $T_K^e > T_K^{o1} > T_K^{o2}$. We note that the last condition has been chosen just for the sake of simplicity, and arbitrary relations among Kondo temperatures can be considered straightforwardly with \mathcal{J}_a presented earlier. As explained above, we consider the 3T Kondo setup in the presence of the Zeeman field B . The case with $B > T_K^e$ results in the weak-coupling regime of the problem. Decreasing B below T_K^e subsequently results in two intermediate states $T_K^{o2} < T_K^{o1} < B < T_K^e$ and $T_K^{o2} < B < T_K^{o1} < T_K^e$. Further decreasing of B finally reaches the strong-coupling regime $B < T_K^{o2}$. In these ways, after three stages of screening of the $S = 3/2$ impurity spin by three conduction channels $\mathcal{K} = 3$, a Kondo singlet is formed at the strong-coupling regime. While the weak-coupling and intermediate-coupling regimes can be understood in terms of well-known perturbative results [18], the strong-coupling regime where all three Kondo channels are at resonance contains most of the non-trivial physics. Therefore, in the following, we develop the transport description at the strong-coupling regime of the 3SK impurity based on a local Fermi-liquid theory.

Scattering theory and conductance matrix. We describe the transport at the strong-coupling regime of the 3SK effect by the celebrated Nozières FL theory [2] which allows us to express all of the scattering effect in terms of three scattering phase shifts $\delta_{a\sigma}$ corresponding to three screening channels per spin projection σ . The idea is to write the scattering matrix $\mathcal{A}_\sigma = \text{diag}[e^{2i\delta_{a\sigma}}]$ for the three-terminal geometry $a = 1, 2, 3$ in the channel (rotated) diagonal basis as in Ref. [40]. From the unitary operator $\mathbb{U}(\varphi)$ Eq. (7) and \mathcal{A}_σ , one then forms a scattering matrix characterizing the transport at the zero-temperature limit,

$$\mathbb{S}(\varphi) \equiv \mathbb{U}^\dagger(\varphi) \mathcal{A}_\sigma \mathbb{U}(\varphi). \quad (11)$$

The Landauer formula then expresses the conductance elements [41]

$$G_{\alpha\alpha'}(\varphi) = \frac{e^2}{h} \sum_{\sigma} |\mathbb{S}_{\alpha\alpha'}(\varphi)|^2, \quad (12)$$

where e is the electron charge and h is the Planck's constant. Equation (12) results in the conductance elements defined in the unit of $G_0 = 2e^2/h$ as

$$G_{12} = \sum_{\sigma} \left[4\mathcal{A}_1 \sin^2 \delta_{12\sigma} + \frac{\mathcal{A}_2}{2} \sin^2 \delta_{23\sigma} - 4\mathcal{A}_3 \sin^2 \delta_{13\sigma} \right],$$

$$G_{13} = G_{23} = 8\mathcal{A}_3 \sum_{\sigma} \sin^2 \delta_{13\sigma}, \quad \delta_{ij\sigma} \equiv \delta_{i\sigma} - \delta_{j\sigma}. \quad (13)$$

The other elements of the conductance matrix are expressible from the above presented elements by using the current conservation at each terminal and symmetry of the conductance elements. In the last equation, we defined the φ dependent factors $\mathcal{A}_i(\varphi)$,

$$\mathcal{A}_1 = \frac{1}{\mathcal{C}^2 + 4\mathcal{C} + 12}, \quad \mathcal{A}_2 = (\mathcal{C} + 2)^2 \mathcal{A}_1, \quad \mathcal{A}_3 = \mathcal{A}_1 \mathcal{A}_2.$$

If all three channels are at resonance, the Friedel sum rule guarantees that the corresponding phase shift becomes $\delta_{i\sigma} = \pi/2$. Equation (13) then accounts for the completely destructive interference among three resonance channels, thereby vanishing the conductance elements. At finite Zeeman field B , the phase shift deviates from the unitary limit. The effects of finite $B \ll T_K^{o2}$ on the conductances are accounted for by the phase shift expansion based on the Nozières FL theory [2,42–44],

$$\delta_{a\sigma} = \frac{\pi}{2} - \bar{\sigma} \alpha_a B, \quad \alpha_a \simeq \frac{1}{T_K^a}. \quad (14)$$

The last equation provides the conductance element G_{12} (in the unit of G_0) of the 3SK effect as

$$G_{12}(\varphi, B) = 8\mathcal{A}_1 \left(\frac{B}{T_K^e} - \frac{B}{T_K^{o1}} \right)^2 + \mathcal{A}_2 \left(\frac{B}{T_K^{o1}} - \frac{B}{T_K^{o2}} \right)^2 - 8\mathcal{A}_3 \left(\frac{B}{T_K^e} - \frac{B}{T_K^{o2}} \right)^2, \quad (15)$$

and similarly for other conductance and reflectance elements. All the features of two-stage and single-stage Kondo effects can be directly seen from Eq. (15). Namely, for $\varphi = 0$, the phase dependent parameter $\mathcal{C}(\varphi = 0) = 0$ and only the Kondo temperature of the even mode is nonzero $T_K^e \neq 0$. This describes the $S = 1/2$ Kondo impurity in 3T geometry with all the conductance elements being equal, $G_{\alpha\alpha'} = 4(B/T_K^e)^2/9$. Straightforward tuning of φ also results in $T_K^{e,o1} \neq 0$ with $T_K^{o2} = 0$, which fully recovers the properties of two-stage Kondo effects.

The parallel configuration of higher-spin Kondo effects in multiterminal geometry results in just the additive contribution to the conductance $G_{3\text{SK parallel}} = 6e^2/h$, and the corresponding series setups are very different with $G_{3\text{SK series}} = \sum_{a \neq a'} \mathcal{L}_{aa'} [\alpha_a(\varphi) - \alpha_{a'}(\varphi)]^2 B^2$. The factors $\mathcal{L}_{aa'}$ are tunable either by phase φ or by tunneling asymmetry. We note that the naive expectation of conductance for 3SK effects, $G_{3\text{SK}} = \text{const} \sum_{a \neq a'} [\alpha_a - \alpha_{a'}]^2 B^2$, is no longer correct, where the consistent description must find $\mathcal{L}_{aa'}(\varphi)$ and $\alpha_a(\varphi)$ carefully as we presented earlier. The calculation at finite temperature and voltage should be performed based on the low-energy FL Hamiltonian presented in SM [35] (which is left for future work).

The intermediate- and weak-coupling regimes of 3SK can be studied straightforwardly with the help of the above presented results and the well-known logarithmic decay of conductance at the weak-coupling regime [37]. Namely, replacing the phase shifts appearing in our expression of conductance elements by [33]

$$\delta_a(B) = \begin{cases} \text{const} \frac{S}{\ln(B/T_K^a)}, & B \gg T_K^a, \\ \text{const} \left[1 - \frac{S}{\ln(T_K^a/B)}\right], & B \ll T_K^a, \end{cases} \quad (16)$$

provides full access to uncover the transport descriptions at the intermediate- and weak-coupling regimes. All the features of 2SK and 1SK effects are thus captured by the 3SK model presented here, in addition to providing different insights on the Kondo paradigm associated with high-spin states. Therefore, the independent control of interfering Kondo channels and their interplay with each other might provide an effective way of using the 3SK setup as a quantum interferometer (further details have been presented in SM).

Summary. We presented a simple description of the multistage Kondo effect in multiterminal geometry based on the Nozières Fermi-liquid theory. The studied framework describes intrinsically multiterminal effects and allows for a precise discrimination between different configurations of the electron states. This provides an access to very rich physics beyond the commonly studied two-terminal and one- or two-mode Kondo screening. We uncovered various, albeit

simple, ways of fine-tuning the multiresonant Kondo channels and their interplay with each other in order to observe the constructive/destructive interference in the simplest possible setup. This minimal setup of the three-stage Kondo effect can be used as a quantum interferometer which also contains all the physics associated with the two-terminal Kondo paradigm and at the same time allows a straightforward generalization to other numbers of stages. The developed framework provides a controllable way to construct a desired realization of the Kondo effect with a particular number of stages, terminals, and channels from combinations of elementary “building blocks,” conceptually alike to making complicated constructions from simple blocks (consequently referred to as a modular quantum interferometer—see Fig. 1). The studied transport observables are within the reach of existing experimental setups, such as of the recent experiment on 2SK effects [7]. Therefore, we believe that the presented ideas would motivate further experiments as well as theoretical works to uncover the Kondo paradigm with high-spin states.

Acknowledgments. We are thankful to J. von Delft and S.-S. Lee for inspiring discussions. The work of M.N.K. is conducted within the framework of the Trieste Institute for Theoretical Quantum Technologies (TQT). M.N.K. appreciates the hospitality of the Physics Department, Arnold Sommerfeld Center for Theoretical Physics and Center for NanoScience, Ludwig-Maximilians-Universität München, where part of this work has been performed.

-
- [1] J. Kondo, *Prog. Theor. Phys.* **32**, 37 (1964).
 - [2] P. Nozières, *J. Low Temp. Phys.* **17**, 31 (1974).
 - [3] A. Hewson, *The Kondo Problem to Heavy Fermions* (Cambridge University Press, Cambridge, UK, 1993).
 - [4] D. L. Cox and A. Zawadowski, *Adv. Phys.* **47**, 599 (1998).
 - [5] P. Nozières and A. Blandin, *J. Phys* **41**, 193 (1980).
 - [6] I. V. Borzenets, J. Shim, J. C. H. Chen, A. Ludwig, A. D. Wieck, S. Tarucha, H.-S. Sim, and M. Yamamoto, *Nature (London)* **579**, 210 (2020).
 - [7] X. Guo, Q. Zhu, L. Zhou, W. Yu, W. Lu, and W. Liang, *Nat. Commun.* **12**, 1566 (2021).
 - [8] P. Simon and I. Affleck, *Phys. Rev. B* **68**, 115304 (2003).
 - [9] M. Pustilnik and L. I. Glazman, *Phys. Rev. Lett.* **87**, 216601 (2001).
 - [10] S. Sasaki, S. De Franceschi, J. M. Elzerman, W. G. van der Wiel, M. Eto, S. Tarucha, and L. P. Kouwenhoven, *Nature (London)* **405**, 764 (2000).
 - [11] W. G. van der Wiel, S. De Franceschi, J. M. Elzerman, S. Tarucha, L. P. Kouwenhoven, J. Motohisa, F. Nakajima, and T. Fukui, *Phys. Rev. Lett.* **88**, 126803 (2002).
 - [12] D. B. Karki and M. N. Kiselev, *Phys. Rev. B* **103**, L201402 (2021).
 - [13] H. Kiyama, K. Yoshimi, T. Kato, T. Nakajima, A. Oiwa, and S. Tarucha, *Phys. Rev. Lett.* **127**, 086802 (2021).
 - [14] L. I. Glazman and M. E. Raikh, *J. Exp. Theor. Phys.* **27**, 452 (1988).
 - [15] T. Numata, Y. Nisikawa, A. Oguri, and A. C. Hewson, *Phys. Rev. B* **80**, 155330 (2009).
 - [16] T. Numata, Y. Nisikawa, A. Oguri, and A. C. Hewson, *J. Phys.: Conf. Ser.* **150**, 022067 (2009).
 - [17] C. B. M. Hørig, C. Mora, and D. Schuricht, *Phys. Rev. B* **89**, 165411 (2014).
 - [18] D. B. Karki, C. Mora, J. von Delft, and M. N. Kiselev, *Phys. Rev. B* **97**, 195403 (2018).
 - [19] D. B. Karki and M. N. Kiselev, *Phys. Rev. B* **98**, 165443 (2018).
 - [20] M. Hanl, A. Weichselbaum, J. von Delft, and M. Kiselev, *Phys. Rev. B* **89**, 195131 (2014).
 - [21] C. Nayak, M. P. A. Fisher, A. W. W. Ludwig, and H. H. Lin, *Phys. Rev. B* **59**, 15694 (1999).
 - [22] G. Benenti, G. Casati, K. Saito, and R. S. Whitney, *Phys. Rep.* **694**, 1 (2017).
 - [23] S. Y. Cho, H.-Q. Zhou, and R. H. McKenzie, *Phys. Rev. B* **68**, 125327 (2003).
 - [24] T. K. T. Nguyen and M. N. Kiselev, *Phys. Rev. Lett.* **125**, 026801 (2020).
 - [25] R. Leturcq, L. Schmid, K. Ensslin, Y. Meir, D. C. Driscoll, and A. C. Gossard, *Phys. Rev. Lett.* **95**, 126603 (2005).
 - [26] M. Büttiker, *Phys. Rev. B* **46**, 12485 (1992).
 - [27] B. Béri and N. R. Cooper, *Phys. Rev. Lett.* **109**, 156803 (2012).
 - [28] T. L. Schmidt, A. Komnik, and A. O. Gogolin, *Phys. Rev. Lett.* **98**, 056603 (2007).
 - [29] K. Kikoin, M. Kiselev, and Y. Avishai, Dynamical symmetries in the Kondo effect, in *Dynamical Symmetries for Nanostructures* (Springer, Vienna, 2011), pp. 107–196.
 - [30] P. W. Anderson, *Phys. Rev.* **124**, 41 (1961).
 - [31] H. R. Krishna-murthy, J. W. Wilkins, and K. G. Wilson, *Phys. Rev. B* **21**, 1003 (1980).

- [32] A. Posazhennikova and P. Coleman, *Phys. Rev. Lett.* **94**, 036802 (2005).
- [33] A. Posazhennikova, B. Bayani, and P. Coleman, *Phys. Rev. B* **75**, 245329 (2007).
- [34] P. Coleman, *Introduction to Many-Body Physics* (Cambridge University Press, Cambridge, UK, 2015).
- [35] See Supplemental Material at <http://link.aps.org/supplemental/10.1103/PhysRevB.105.L041410> for additional details for the derivation of key equations presented in this Letter.
- [36] J. R. Schrieffer and P. Wolf, *Phys. Rev.* **149**, 491 (1966).
- [37] M. Pustilnik and L. Glazman, *J. Phys.: Condens. Matter* **16**, R513 (2004).
- [38] J. B. Bronzan, *Phys. Rev. D* **38**, 1994 (1988).
- [39] H. Georgi, *Lie Algebras in Particle Physics: From Isospin to Unified Theories*, Frontiers in Physics Vol. 54, 2nd ed. (CRC Press, Boca Raton, FL, 2018).
- [40] M. Pustilnik and L. I. Glazman, *Phys. Rev. B* **64**, 045328 (2001).
- [41] R. Landauer, *IBM J. Res. Dev.* **1**, 223 (1957).
- [42] C. Mora, P. Vitushinsky, X. Leyronas, A. A. Clerk, and K. Le Hur, *Phys. Rev. B* **80**, 155322 (2009).
- [43] C. Mora, *Phys. Rev. B* **80**, 125304 (2009).
- [44] C. Mora, C. P. Moca, J. von Delft, and G. Zaránd, *Phys. Rev. B* **92**, 075120 (2015).